Earthquake Engineering, Tenth World Conference © 1992 Balkema, Rotterdam. ISBN 90 5410 060 5

Evaluation of cracked and repaired beams and columns using surface stress waves

Britt R. Bowen
United States Air Force, USA

Kenneth H. Stokoe II
The University of Texas at Austin, Tex., USA

Abstract: The Spectral-Analysis-of-Surface-Waves (SASW) method is a nondestructive seismic method which has been used in situ to determine the elastic moduli of soils and pavements at low levels of strain and the variation of these moduli with depth. In this work, applicability of the SASW method to the identification of (1) sound concrete, (2) cracks in concrete members, and (3) the quality of crack repair was investigated. Results are presented from experimental studies on small-scale beams and one full-scale column which show that the SASW method can be used to evaluate these structural conditions.

1 INTRODUCTION

The Spectral-Analysis-of-Surface-Waves (SASW) method is an established seismic method for in situ nondestructive testing of soils and pavements (Nazarian and Stokoe, 1988; Stokoe et al, 1988). Recently, the method has been adapted for use on curing and cured concrete slabs (Bay and Stokoe, 1992). In these cases, a source and two receivers are placed on the exposed surface of the material system to be tested as illustrated in Figure 1. The source imparts a vertical impulse to the system which creates surface seismic (stress) waves of the Rayleigh type that propagate away from the source. The receivers record vertical particle velocities or accelerations at two points on the surface created by the surface waves propagating away from the source. The distance from the source to the first receiver, d_1, is normally kept equal to the distance between receivers, Δd. Analytical studies (Sanchez Salinero, 1987) have shown that the best arrangement of the source to the first receiver for reliable interpretation of surface wave propagation occurs when the distance, d_1, is greater than about one wavelength (λ_R).

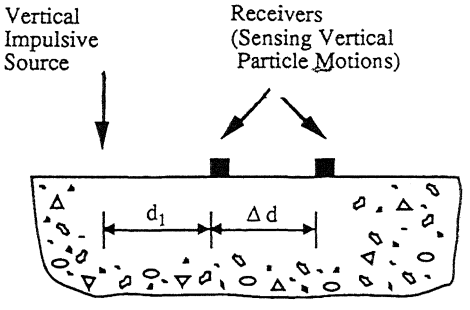

Figure 1 General arrangement of source and receivers used in SASW testing.

The objective of the test is to determine the surface wave dispersion curve for the material being tested. The dispersion curve is a plot of wave velocity, V_R, versus frequency, f, or wavelength, λ_R. To calculate the dispersion curve, the cross-power spectrum of the motions recorded by the two receivers is determined from which one finds the phase difference, $\phi(f)$, between these motions as a function of frequency. The apparent velocity of propagation of the surface wave for each frequency, $V_R(f)$, is then simply:

$$V_R(f) = (2\pi f \Delta d) / \phi(f) \qquad (1)$$

with the phase for each frequency, $\phi(f)$, in radians. The wavelength, λ_R, is simply the velocity divided by the frequency.

Surface waves and the SASW method have several features which makes the technique attractive. They include: (1) When an impact on the surface is used to create the stress waves, the majority of the energy from the impact is imparted in surface waves, with the remainder going into body waves. (2) The damping due to geometrical spreading for surface waves (cylindrical spreading) is smaller than for body waves (spherical spreading). (3) The SASW method only requires access to one side of the member. (4) The surface wave dispersion curve also provides information about the variation of stiffness with depth into the beam due to the dispersive nature of the surface wave which results in different wavelengths sampling different depths.

The purpose of the study reported herein was to assess the applicability of the SASW method to concrete structural members for evaluation of: (1) concrete soundness, (2) crack detection and (3) repair quality. To do this, small-scale tests were performed to apply the method to beam elements and to study how cracks affect the dispersion curve. In addition, a full-scale column was tested to study the effectiveness of the method to the detection of damage as cyclic loading progresses.

2 SMALL-SCALE BEAMS

2.1 *Test set-up and equipment*

SASW tests were performed on 53.3 cm x 15.2 cm x 15.2 cm specimens which were made of cement and sand with no coarse aggregate. Theses small-scale beams were simply supported, resting on steel cylindrical rods placed under the ends of the specimens. Tests were conducted using different receiver spacings, Δd, of 3.8 cm, 7.6 cm, and 15.2 cm. For each spacing, tests were conducted along the centerline on the top surface of the beam by moving the source and receivers along the beam. SASW tests were performed first on an intact beam and then on beams with a 2.5-cm, 5.1-cm or 7.6-cm deep crack at midspan. The cracks were vertically oriented and were cut in each beam, starting at the beam surface. Figure 2 shows schematically these various arrangements of the source, receivers and "manufactured" cracks.

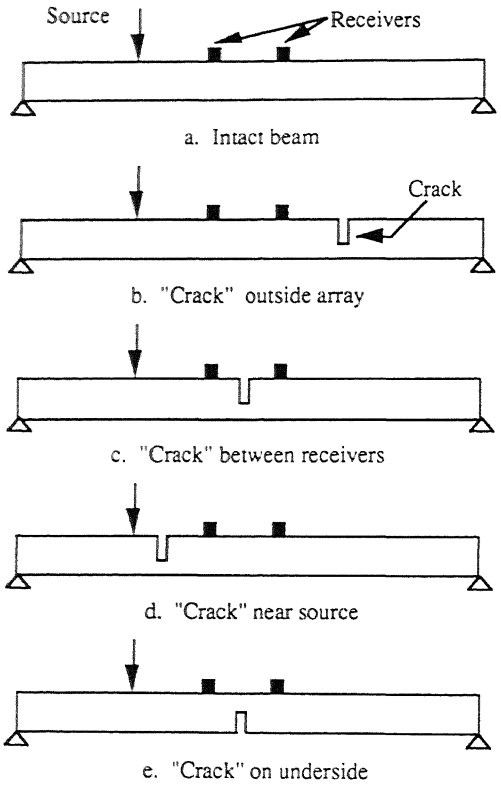

Figure 2 Arrangements of source, receivers and "manufactured" cracks in small-scale beam tests.

An instrumented hammer or ball bearings were used as the source. Miniature accelerometers were used as receivers. A Hewlet-Packard Model 3562A Dynamic Signal Analyzer was used to record the accelerometer outputs and to perform waveform analyses. The data were stored on a 8.9-cm floppy disk via an HP9122 disk drive.

2.2 *Intact beam (Figure 2a)*

Based on initial tests with the intact small-scale beam, a 7.6-cm receiver spacing was found to work well. A typical phase diagram is shown in Figure 3a when testing with this receiver spacing. The resulting dispersion curve using Eq. 1 with Figure 3a is shown in Figure 3b.

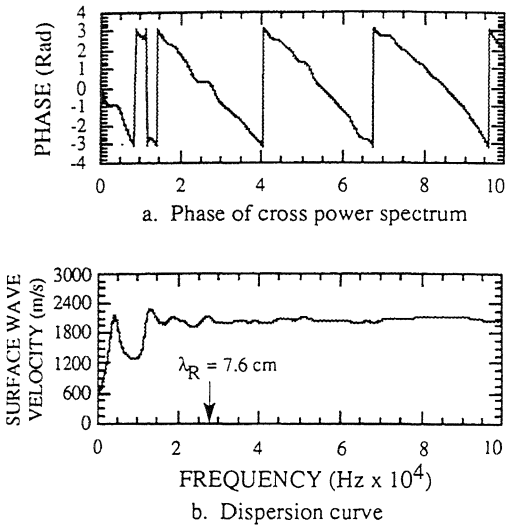

Figure 3 Typical SASW results: Intact beam and 7.6-cm receiver spacing.

The experimental results show that for wavelengths smaller than half the depth of the beam (which corresponds to 7.6 cm or less), the surface wave velocity is essentially constant. These wavelengths are represented by frequencies equal to or greater than about 28 kHz in Figure 3b. For wavelengths greater than half the depth of the beam, the trend in the dispersion curve is for velocity to decrease with increasing wavelength. However, the velocity shows large fluctuations in this trend as seen in Figure 3b below a frequency of 28 kHz. This dispersive behavior corresponds closely with the analytical solution for the Rayleigh wave speed in a uniform layer of finite thickness with air on both sides (Bowen, 1992). The analytical solution predicts a phase velocity which is essentially constant for wavelengths smaller than half the depth of the beam and nearly so for wavelengths up to the depth of the beam. For larger wavelengths (smaller frequencies) the velocity decreases considerably.

The constant value of velocity in the dispersion curve for frequencies greater than 28 kHz indicates that the concrete in the upper half of the beam is uniform. The constant velocity can be used to calculate the modulus of elasticity by:

$$E = 2\,(1 + \nu)\,\rho\,V_S^2 \qquad (2)$$

were ρ is the material mass density, ν is Poisson's ratio, and V_S is the shear wave velocity of the concrete.

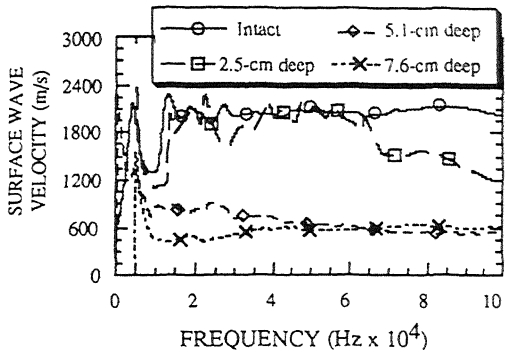

Figure 5 Dispersion curves for small-scale beams with no damage and with a crack between receivers: 7.6-cm receiver spacing.

For a given material, the Rayleigh wave velocity, V_R, and the shear wave velocity, V_S, can be expressed as a ratio, V_S/V_R, which is a function of Poisson's ratio as:

$$V_S \cong V_R\,(1 + \nu)/(0.87 + 1.12\nu) \qquad (3)$$

For sound concrete, V_S/V_R ranges from about 1.09 to 1.11. Using this relationship, V_S is calculated from the measured value of V_R, which is then used to calculate the modulus of elasticity using Eq. 2.

For this example, a Rayleigh wave velocity of 2100 m/s was selected as an average of the values for frequencies above 28 kHz, and a Poisson's ratio of 0.20 was assumed. The resulting Young's modulus is about 30 x 10^6 kN/m^2 which is typical of sound concrete at small strains. Hence, the value of the Rayleigh wave velocity or Young's modulus can be used as one indicator of concrete quality.

2.3 *Crack outside source-receiver array (Figure 2b)*

When the crack is not in the travel path between the source and the second receiver, the crack does not affect the measured dispersion curve. In this case, the same results presented in Figure 3 are measured and uniform, sound concrete is determined in the upper half of the beam.

2.4 *Crack between receivers (Figure 2c)*

In Figures 4b, 4c, and 4d, the phase diagrams are shown for testing performed on the small-scale beams with vertical cracks located between the two receivers and on the same face (Figure 2c). The receiver spacing was 7.6 cm, and the second receiver was placed just past the crack. As seen in the phase diagrams, the crack affects the measurements by adding additional cycles of phase, and the fact that the beam is not intact is immediately evident.

Figure 5 shows the subsequent experimental dispersion curves derived from the phase diagrams. When the dispersion curve is calculated for the cases with a crack, there is a clear decrease in the phase

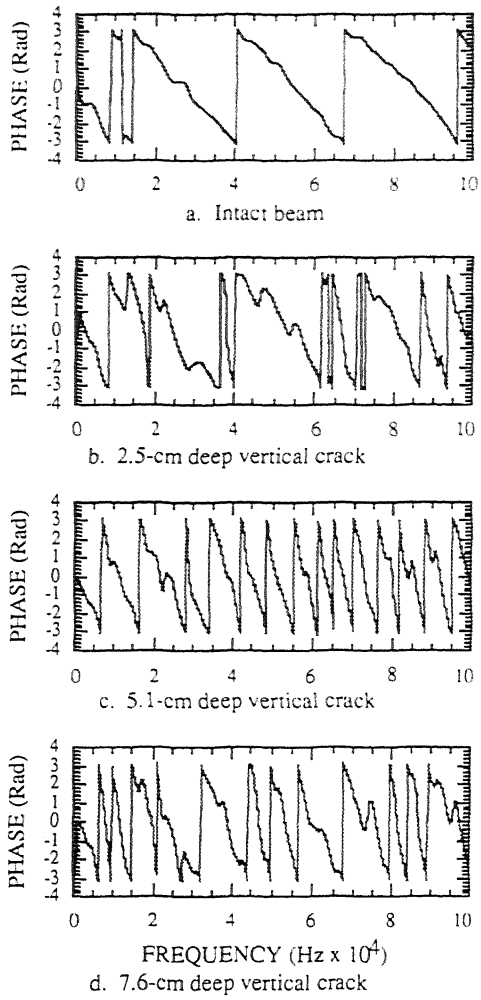

Figure 4 SASW phase diagrams for small-scale beams with no damage and with a crack between receivers: 7.6-cm receiver spacing.

velocity for the cracked beams, indicating damaged or poor concrete. Interestingly, the dispersion curve for the beam with a 2.5-cm deep crack shows that concrete below the crack is sound.

2.5 *Crack between source and first receiver (Figure 2d)*

When the crack is between the source and first receiver, the phase diagram is also affected. The phase diagram from the cracked sections are more complex than for the intact beam (Figure 4a) and appear to exhibit fewer cycles of phase than measured for the intact beam. Less phase shift results in unreasonably high velocities in the dispersion curve, above 3000 m/s. These unreasonably high velocities turn out to be the indicator of damaged concrete.

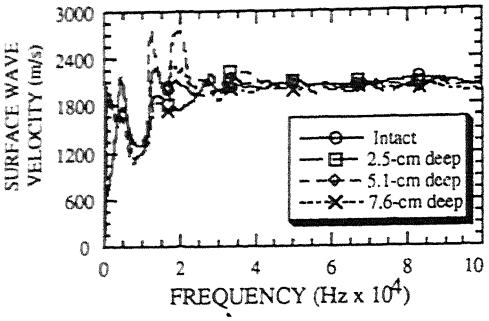

Figure 7 Dispersion curves for repaired beams: 3-in. receiver spacing and crack between receivers.

2.6 *Crack on the underside (Figure 2e)*

The only condition tested with a crack on the underside of the beam was when the crack was located between the receivers (Figure 2e) and a 7.6-cm receiver spacing was used. In this case, the measured dispersion curve was not affected because all wavelengths were equal to or less than half the depth of the beam.

3 REPAIRED SMALL-SCALE BEAMS

After the small-scale beams were tested with the "manufactured" cracks, the cracks were repaired by filling the cracks with Quickcrete - Fast Setting Cement. The beams were retested only by locating the repaired cracks between the receivers. The resulting dispersion curves from the repaired beams were similar to those for the undamaged case for the 7.6-cm and 15.2-cm receiver spacings.

Figure 6 shows the experimental phase diagrams for the beam with no damage and the repaired beams. These measurements were made in the same location as those presented in Figure 4 when the beams had the "manufactured" cracks. Figure 7 shows the subsequent experimental dispersion curves. The dispersion curves for the repaired beams, where the second receiver was just past the repair, give the same velocities as the undamaged beam, indicating a good repair. However, the strength of the repair cannot be determined by small-strain measurements such as these.

4 FULL-SCALE COLUMN

4.1 *Test set-up*

A full-scale column was also tested. As shown in Figure 8, the column was loaded at the top, perpendicular to the column centerline. The column was loaded in cycles, with two cycles at each load level. Each cycle started at zero load. The column was then pushed to a given load level, the load was removed, and the column was then pulled to the same load level and finally returned to zero load. This loading sequence was considered to be one cycle. The first load was 22.2 kN and was increased in 22.2-kN increments for each subsequent load level to a final load level of about 222 kN.

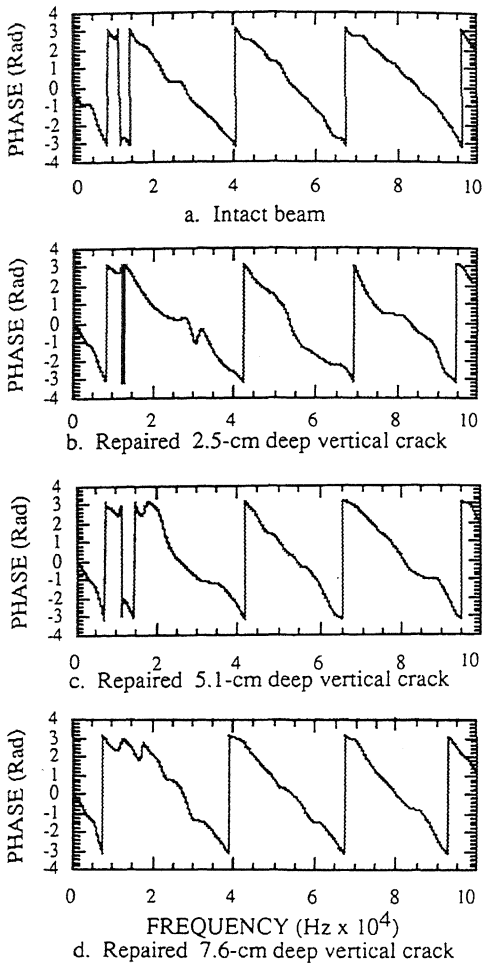

Figure 6 Phase diagrams for repaired small-scale beams: 7.6-cm receiver spacing and crack between receivers.

The column was 0.46 m x 0.92 m x 2.75 m. The column was spliced to a foundation using 16, #8 rebar (2.5-cm diameter), with 8 bars along each 0.92-m wide face. The splice reinforcement extending out of the foundation was also #8 rebars and extended 0.61 m above the foundation. The longitudinal bars overlapped the entire 0.61 m and extended to the top of the column. The concrete cover was 3.8 cm. A cold joint between the foundation and bottom of the column was formed during the construction process.

SASW measurements were made vertically on the 0.92-m wide face at a distance of 0.24 m from the edge (between the longitudinal reinforcement). These measurements were performed in the general location of the top of the splice as shown in Figure 8. Both 15.2-cm and 22.9-cm receiver spacings were used. As the column was cycled, the testing face alternated between tension and compression states of stress. SASW measurements were performed at the maximum compression and tension stresses in each cycle.

4.2 *Measurement complications*

In the small-scale beam tests, there was neither *reinforcement nor coarse aggregate. In the full-scale* tests, both are present which complicates the measurement. The aggregate size limits the smallest wavelength which can be measured. The maximum aggregate size in the column was 1.6 cm. For the configuration of reinforcement shown in Figure 8, the reinforcement caused no problem in the measurements when testing along the centerline of the 0.46-m wide face. When testing on the 0.92-m wide face, the reinforcement did affect the measurements in the high frequency or short wavelength range. This was true when testing directly over and parallel to the reinforcement as well as when testing parallel to the reinforcement and along a centerline between two adjacent reinforcing bars. In both cases, for the aggregate and the reinforcement, the effect was the same; that is to limit the highest frequency to about 50 kHz and the shortest wavelength to about 4.1 cm.

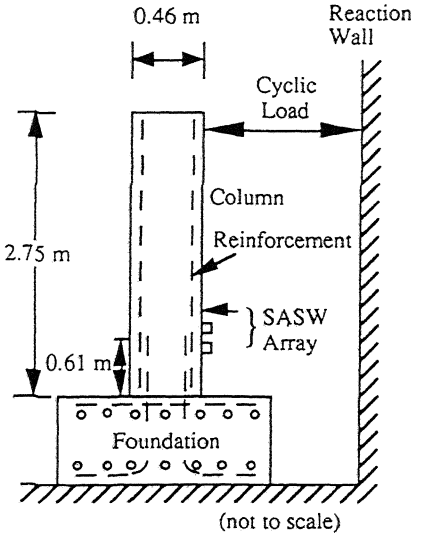

Figure 8 Test configuration used in SASW measurements of full-scale column loaded cyclically.

4.3 *Load progression*

Only data from the first cycle at each load level when the face was in tension are shown. When the face was in compression, any cracks were pushed together and there was little difference in the dispersion curves at the progressive load levels. Further investigation of the attenuation characteristics under compression loading is underway.

Figure 9 shows the phase diagrams for the source-receiver array parallel and between the reinforcement. Testing was performed on the 0.92-m wide face with a 15.2-cm receiver spacing. These measurements were performed at progressively higher loads. For load levels between 0 and 66.7 kN, the measured dispersion curves did not change. As such, the phase diagram

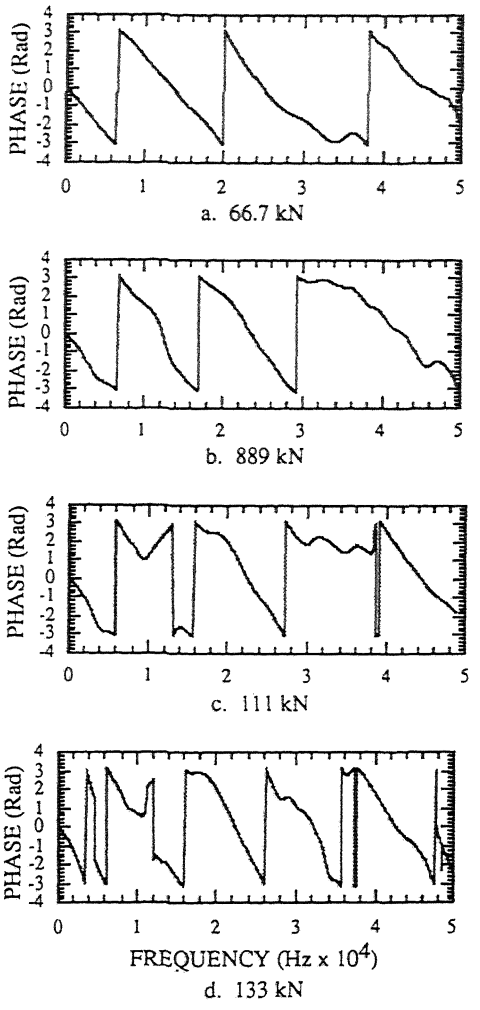

Figure 9 Phase diagrams on full-scale column at progressively higher loads: 15.2-cm receiver spacing and receivers on tension face in the location of the splice.

measured under a peak load of 66.7 kN (Figure 9a) is used as the baseline phase diagram for comparison purposes. At the 89-kN load level, the phase diagram (Figure 9b) began to differ from the 66.7-kN phase diagram. The phase diagram for the 89-kN load level exhibits greater phase shifts than the 66.7-kN phase diagram at frequencies above about 10 kHz. This results in a slowing of the apparent surface wave velocities of approximately 120 m/s over the frequency range of *10 to 50 kHz* as shown in the dispersion curves in Figure 10. Up to this load level, no cracks were noticed in the path between the source and receivers. However, this slight reduction in Rayleigh wave velocities indicates that damage has just started, even though no cracks could be seen.

At the 111-kN load level, the phase diagram (Figure 9c) became quite different from the phase diagram

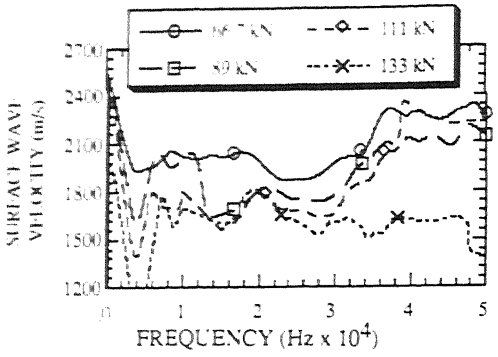

Figure 10 Dispersion curves of no damage and a crack between the receivers on the full-scale column: 15.2-cm receiver spacing and testing on the tension face.

measured under a load of 66.7 kN. A crack was visible between the receivers at this load level. The subsequent dispersion curve (Figure 10) showed the Rayleigh wave velocities decreased by about 120 to 400 m/s in the frequency range of 5 to 40 kHz.

At the 133-kN load level, the phase diagram (Figure 9d) continued to become increasingly different from the phase diagram measured under a load of 66.7 kN. In this case, two cracks were visible, one between the source and first receiver, and the crack between the two receivers seen at a load of 111 kN. The average value of the Rayleigh wave velocity is about 1650 m/s at this time as seen in Figure 10. Clearly, this value is indicative of damaged concrete because it is about 20 to 25% less than the wave velocities measured in the undamaged column. This decrease in wave velocity represents about a 35 to 45% decrease in Young's modulus. SASW testing was discontinued after this load level due to repairs required in the loading equipment.

5 SUMMARY

The Spectral-Analysis-of-Surface-Waves (SASW) method is a nonintrusive seismic method which can be used to determine the variation of stiffness (Young's modulus) with depth into a concrete beam or column. One attractive feature of the method is that access to only one side of the structural element is required. Measurement of Rayleigh-type surface waves propagating along the surface of the structural element is performed with a source and two receivers placed on the exposed surface. The measurement results in calculation of a dispersion curve which is a plot of Rayleigh wave velocity versus frequency or wavelength. Sound concrete elements are identified by dispersion curves which exhibit a nearly constant wave velocity with wavelength, with Rayleigh wave velocities typically in the range of 2000 to 2200 m/s. Changes in the dispersion curve between sound, damaged and repaired states are used to evaluate damage and repair.

SASW tests were performed on intact and "cracked" small-scale beams to study the influence of cracks. The small-scale beam tests showed that a crack between the receivers caused the apparent surface wave velocity to decrease. On the other hand, a crack between the source and first receiver resulted in the apparent surface wave velocity increasing to unrealistically high values. Other source-receiver-crack configurations did not show any difference in the dispersion curve. Hence, cracks or damage can be located by moving the SASW array along the structural element and locating those areas where change in the dispersion curve occur.

The small-scale "cracked" beams wre also repaired. SASW tests on the repaired beams showed that the dispersion curve measured on an undamaged cross-section and those measured on the repaired cross-sections exhibited no difference, indicating good repair. However, the strength of the repair could not be evaluated by these small-strain stress wave measurements.

SASW tests were also performed on a full-scale column which was subjected to cyclic loading. Damage to the concrete when the column face was in tension was detected in the dispersion curves somewhat before visible cracking was noted. The dispersion curves indicated significant damage to the concrete at the same time visible cracking was noted. However, the SASW tests showed little change in wave velocity when the cracked face was in compression. Further work is necessary to evaluate the attenuation characteristics when cracks are under compressive loads and to evaluate crack depth from the dispersion curves.

ACKNOWLEDGMENTS

The work described herein was conducted as part of a research project sponsored by the National Science Foundation (NSF) under Grant Number MSS-9018962. Special thanks goes to Dr. M. Tumay of NSF for his support and encouragement. Drs. J. Roesset and J. Jirsa are co-investigators on this research project and their guidance is sincerely appreciated. Thanks also goes Dr. M. Englehart and Mr. R. Aboutaha for allowing us to test the full-scale column.

REFERENCES

Bay, J.A. and Stokoe, K.H., II. 1992. Field and Laboratory Determination of Elastic Properties of PCC Using Seismic Techniques. Transportation Research Board Annual Meeting Preprint No. 920749, Washington, D.C., 1992 (accepted for publication).

Bowen, B. 1992. Damage Detection in Concrete Elements with Surface Wave Measurements. Ph.D. Dissertation, The University of Texas at Austin, 188 p.

Nazarian, S., and Stokoe K.H., II. 1988. Nondestructive Evaluation of Pavements by Surface Wave Method. *Proceedings*, American Society for Testing and Materials, ASTM STP 1026, Philadelphia, Pennsylvania, pp. 119-137.

Stokoe, K.H., II, Nazarian, S., Rix, G.J., Sanchez-Salinero, I., Sheu, J.-C., and Mok, Y.J. 1988. In Situ Seismic Testing of Hard-to-Sample Soils by Surface Wave Method. *Proceedings*, American Society of Civil Engineers, Park City, Utah, pp. 264-278.

Sanchez Salinero I. 1987. Analytical Investigation of Seismic Methods Used for Engineering Applications. Ph.D. Dissertation. The University of Texas at Austin, 401 p.